A new method to suppress the MHD instability of cylindrical liquid metal batteries

Chenhao Li, Ke Liu, Jingru Guo, Benwen Li*

Key Laboratory of Ocean Energy Utilization and Energy Conservation of Ministry of Education, School of Energy and Power Engineering, Dalian University of Technology, Dalian 116024, China

Abstract—The magnetohydrodynamics (MHD) instabilities of liquid metal batteries (LMBs) severely limit the wide application and commercialization of LMB. A new technology is proposed, which is called the grid-structure (GS), so as to achieve the suppression effect of the MHD instabilities in LMB. The GS is composed of electrically and magnetically insulated partitions, which fully contact the negative electrode and extended to the positive electrode of the battery. It is found that the GS inserted inside the LMBs can change the distribution of the circumferential induced magnetic field inside the battery, effectively reduce the induced magnetic field and Lorentz force, and thus improve the stability of the LMB.

1. Introduction

Liquid Metal Batteries (LMBs), as one of the electrochemical energy storage, has the advantages of high energy efficiency, flexibility of power, long life and low maintenance cost, and is considered as an energy storage technology with great potential. However, due to working in high operating temperature, the LMBs are prone to Taylor instability (TI)[1,2], Sloshing instability(SI)[3,4], Rayleigh-Bénard instability (RBI)[5–7] and Electro-Vortex Flows (EVFs)[8–10] and other flow instability, which are called the magnetohydrodynamics (MHD) instability. Therefore it is necessary to suppress the MHD instability in LMBs.

A large number of scholars have studied the internal MHD instability of Liquid Metal Battery (LMB). By simplifying the research model, one or two kinds of instability in the battery have been analyzed and studied, and the methods to restrain such instability have been proposed. However, the MHD flow inside LMB is a more complex flow phenomenon based on the coupling of the above instabilities, which seriously affects the safe and stable operation of batteries and restricts the commercial application of batteries. Therefore, this paper carried out numerical simulation for cylindrical LMB to study its internal instability. At the same time, a new grid structure is proposed, which can restrain the occurrence of instability by changing the spatial distribution of magnetic field and flow field inside LMB, improve the working efficiency of LMB, and avoid the occurrence of short circuit accidents.

2. Physical model and mathematical model

2.1. Physical model

In this paper, the cylindrical physical model of LMBs with height-width ratio of Γ=H/D=4.5 (cell height H=450mm, diameter D=100mm) was established for calculation. The thickness ratio of three layers was 4:1:4, and the thickness of positive electrode, electrolyte and negative electrode materials was h_1=200mm, h_2=50mm and h_3=200mm. As shown in Fig.1, we choose Li||LiCl-KCl||Pb-Bi as the negative, electrolyte and anode materials same as those in Refs. [6]. The top of the grid is in complete contact with the negative current collector. The grid structure is composed of metal plate or metal mesh wrapped with ceramic material, which has the effect of magnetic insulation. The bottom of the grid is lower than the maximum distance that the electrolyte layer moves downward during the battery charging process and extends to the positive electrode material.

* heatli@dlut.edu.cn

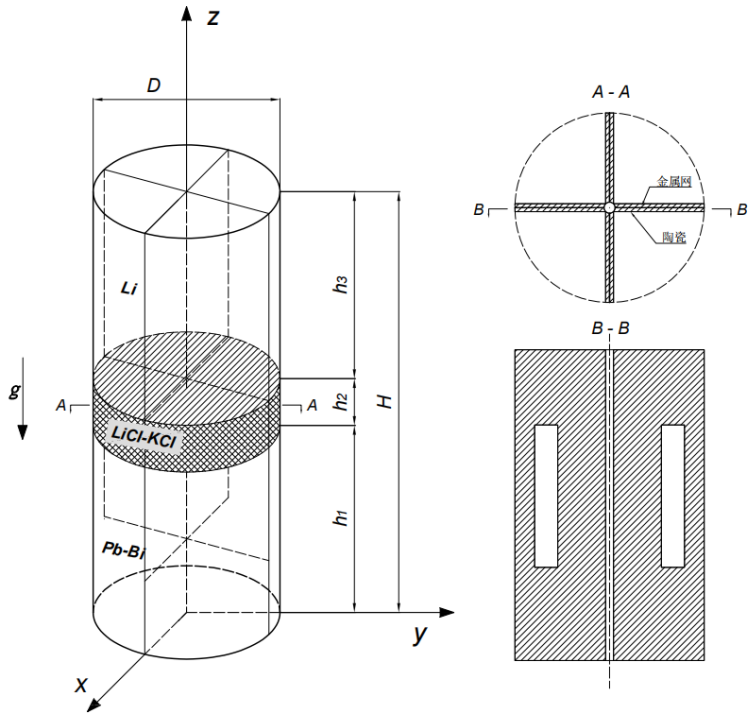

Fig.1. 3D structure of liquid metal battery and its internal grid structure

2.2. Governing equations

The Navier-Stokes and Maxwell equations, in addition to Ohm's law for flowing media, are used to describe the motion of electrically conducting fluid when it is subjected to an electromagnetic field. The momentum equations are described by the Navier-Stokes equations for incompressible fluids:

$$\frac{\partial u_i^{(n)}}{\partial x_i} = 0 \tag{1}$$

$$\frac{Du_i^{(n)}}{Dt} = -\frac{1}{\rho}\frac{\partial p^{(n)}}{\partial x_i} + g + \frac{\partial}{\partial x_j}\left[\nu\left(\frac{\partial u_i^{(n)}}{\partial x_j} + \frac{\partial u_j^{(n)}}{\partial x_i}\right)\right] + \frac{1}{\rho}\varepsilon_{ijk} j_j^{(n)} B_k^{(n)} \tag{2}$$

cathode, electrolyte, and anode, respectively, are denoted by the superscripts n (n = 1, 2, and 3). Where g is the standard gravity, ρ is the density, ν is the kinematic viscosity of single-phase , u is the velocity, p is the pressure, j is the total current density (sum of the applied current and the induced current), B is the induced magnetic field from current density j.

By using the magnetic vector potential (MVP) approach, we may derive the induced magnetic field from the electric potential by solving the MVP equation. As a result, we must first obtain the distribution of the relevant electric potential field. The following is the equation for the electric potential:

$$\sigma_{mag}\nabla^2 E = \nabla \cdot \boldsymbol{U} \times \boldsymbol{B} \tag{3}$$

where, σ_{mag} is the electrical conductivity, E is the electric potential field. The MVP equation is then used to calculate the induced magnetic field, and it is as follows:

$$\nabla \boldsymbol{A}^{(n)} = \mu_0 \sigma_{mag} \nabla E^{(n)} \tag{4}$$

$$\boldsymbol{B}^{(n)} = \nabla \times \boldsymbol{A}^{(n)} \tag{5}$$

We employ the volume-of-fluid (VOF) approach to compute and track the locations of the liquid-liquid interfaces in multiphase flows since it has been used to simulate a wide range of scenarios in research and commercial areas.

3. Results and Discussions

In order to verify the inhibition effect of the grid structure on the internal instability of LMBs, this paper compared the LMBs in the case of added and unadded grilles to verify the inhibition effect of GS. When the battery is at a voltage of 200V, its 3D and 2D morphology maps of the electrolyte layer are shown in Fig.2.

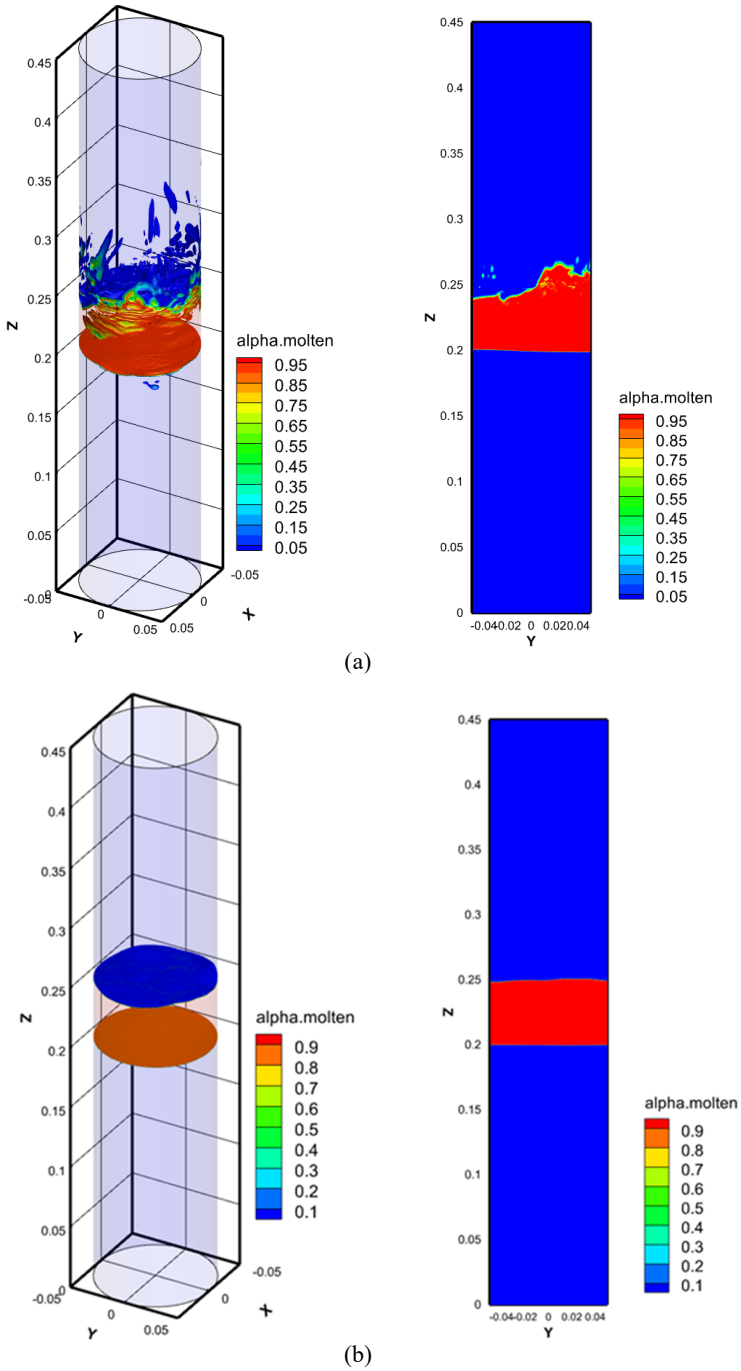

Fig.2. The 3D and 2D morphology maps of LMBs at a voltage of 200V: (a) liquid metal battery without the GS; (b) liquid metal battery which has the GS comprised of four baffles.

As shown in Fig. 2(a), the electrolyte layer of classical LMB without the GS cannot maintain its original shape, and the shape of the red region in the figure changes greatly, and its shape is completely irregular. At this time, a large area of volume fraction α<l is the yellow, green region, which means the beginning of mixing of different fluids in the LMB. In other words, the electrolyte layer, unable to maintain its original form, appears to spray, indicating that the LMB's positive and negative liquid electrodes are connected to each other, indicating a short circuit inside the battery. However, when four baffles was placed in the LMB at 200V, the numerical results are as shown in Fig. 2(b). We can see the interface between the molten salt layer and the other two liquid electrodes is still very smooth, indicating that the battery can still work stably at this time.

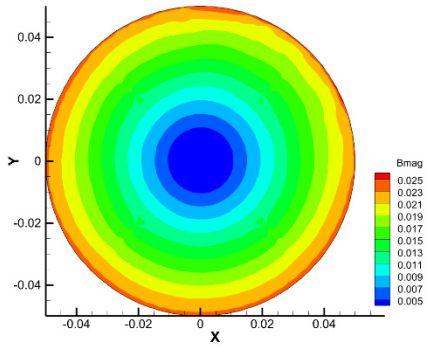

(a)

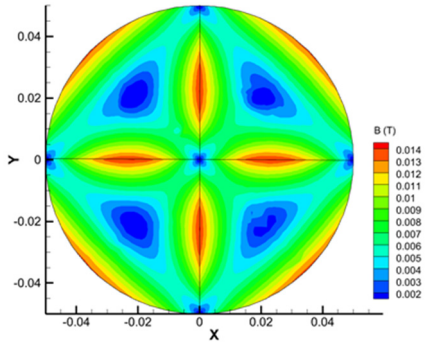

(b)

Fig.3. Cross section induced magnetic field distribution on a XOY plane (E=200V, t=0.2s, z=0.25): (a) induced magnetic field; (b) induced magnetic field (with 4 baffles).

Biot-Savart law shows that, under the same current density, the larger the cross-section of the fluid, the greater the intensity of the induced magnetic field. Fig. 3 shows the strength and distribution of the induced magnetic field inside the LMB on a XOY plane (E=200V, t=0.2s, z=0.25). It was found that the induced magnetic field distribution was divided into four small loops by 4 spacers, and the maximum magnetic field intensity was reduced by half, as shown in Fig. 3(b). The fundamental reason for the variation of magnetic field intensity and distribution lies in the special properties of grid structure. The grid structure is an insulating part. After the grid structure is placed, the current intensity in each small space divided is reduced to 1/4 of the original current intensity. In addition, because of the presence of metal mesh or plate inside the partition, the induced magnetic fields generated in each small space cannot converge. According to Biot-Savart's law, the induced magnetic field strength can be reduced by 50% in each small space. In other words, the grid structure's arrangement significantly reduces the intensity of the induced magnetic field at the fluid interface, which helps to prevent the occurrence of instability, such as TI and SI.

4. Conclusion

Based on the findings and debates described above, the conclusions are drawn as follows:

(1) When the operating voltage is equal to 200V, the Lorentz force inside the battery is greater than the viscous force of the liquid inside the battery, and the interface between the electrolyte layer and the negative electrolyte begins to appear obvious interface fluctuations. At this time, the battery will appear short circuit if it continues to work.

(2) The grid structure (GS) composed of multiple partitions can suppress the instability in LMB. When the number of inserted partitions is 4, the MHD instability of LMBs at 200V voltage is suppressed.

(3) When four grids are inserted into the cell, the induced magnetic field distribution is split into four small loops, and the induced magnetic field intensity in each small space can be reduced by 50%.

Acknowledgment

This work was supported by the National Natural Science Foundation of China with granted No. 51976021 and the Fundamental Research Funds for the Central Universities (DUT21GJ202).

References

1. Weber N, Galindo V, Stefani F. Current-driven flow instabilities in large-scale liquid metal batteries, and how to tame them[J/OL]. Journal of Power Sources, 2014, 265: 166-173. DOI:10.1016/j.jpowsour.2014.03.055.
2. Stefani F, Weier T, Gundrum T. How to circumvent the size limitation of liquid metal batteries due to the Tayler instability[J/OL]. Energy Conversion and Management, 2011, 52(8-9): 2982-2986. DOI:10.1016/j.enconman.2011.03.003.
3. Weber N, Beckstein P, Galindo V. Metal pad roll instability in liquid metal batteries[J/OL]. Magnetohydrodynamics, 2017, 53(1): 129-140. DOI:10.22364/mhd.53.1.14.
4. Horstmann G M, Weber N, Weier T. Coupling and stability of interfacial waves in liquid metal batteries[M/OL]. arXiv, 2017[2022-09-29]. http://arxiv.org/abs/1708.02159.
5. Keogh D F, Timchenko V, Reizes J. Modelling Rayleigh-Bénard convection coupled with electro-vortex flow in liquid metal batteries[J/OL]. Journal of Power Sources, 2021, 501: 229988. DOI:10.1016/j.jpowsour.2021.229988.
6. Köllner T, Boeck T, Schumacher J. Thermal Rayleigh-Marangoni convection in a three-layer liquid-metal-battery model[J/OL]. Physical Review E, 2017, 95(5): 053114. DOI:10.1103/PhysRevE.95.053114.
7. Personnettaz P, Beckstein P, Landgraf S. Thermally driven convection in Li||Bi liquid metal batteries[J/OL]. Journal of Power Sources, 2018, 401: 362-374. DOI:10.1016/j.jpowsour.2018.08.069.
8. Kolesnichenko I, Frick P, Eltishchev V. Evolution of a strong electrovortex flow in a cylindrical cell[J/OL]. Physical Review Fluids, 2020, 5(12): 123703. DOI:10.1103/PhysRevFluids.5.123703.

9. Herreman W, Bénard S, NORE C. Solutal buoyancy and electrovortex flow in liquid metal batteries[J/OL]. Physical Review Fluids, 2020, 5(7): 074501. DOI:10.1103/PhysRevFluids.5.074501.
10. Herreman W, Nore C, Ziebell Ramos P. Numerical simulation of electrovortex flows in cylindrical fluid layers and liquid metal batteries[J/OL]. Physical Review Fluids, 2019, 4(11): 113702. DOI:10.1103/PhysRevFluids.4.113702.